Letter

Energy landscape design principle for optimal energy harnessing by catalytic molecular machines

Zhongmin Zhang , Vincent Du , and Zhiyue Lu [*]

Department of Chemistry, University of North Carolina, Chapel Hill, North Carolina 27599-3290, USA

Under temperature oscillation, cyclic molecular machines such as catalysts and enzymes could harness energy from the oscillatory bath and use it to drive other processes. Using an alternative geometrical approach, under fast temperature oscillation, we derive a general design principle for obtaining the optimal catalytic energy landscape that can harness energy from a temperature-oscillatory bath and use it to invert a spontaneous reaction. By driving the reaction against the spontaneous direction, the catalysts convert low free-energy product molecules to high free-energy reactant molecules. The design principle, derived for arbitrary cyclic catalysts, is expressed as a simple quadratic objective function that only depends on the reaction activation energies, and is independent of the temperature protocol. Since the reaction activation energies are directly accessible by experimental measurements, the objective function can be directly used to guide the search for optimal energy-harvesting catalysts.

In stochastic thermodynamics, catalysts and enzymes can be considered cyclic molecular machines [1–10]: The catalyst undergoes a cycle of state changes to assist the conversion of reactant(s) to product(s), and returns to its initial state. In a stationary environment, the catalytic cycle reaches a nonequilibrium steady state (NESS), driven by the thermodynamically spontaneous reaction ($\Delta G < 0$) to a biased direction.

In idealized stationary environments, molecular machines can transduce free energy from one form to another [11–13]. By contrast, molecular machines in realistic time-varying environments can demonstrate unusual dynamical and thermodynamic behavior beyond NESS. For example, a periodically oscillating environment could drive a detailed-balanced system to mimic a dissipative system [14,15]. Moreover, the driving force provided by the time-changing environment could drive enzymes or molecular complexes to function as engines, ratchets, or pumps [16–28]. Also, periodically oscillating temperatures could drive catalysts to alter the reaction kinetics or even shift the equilibrium concentration [29–31]. These results indicate that catalysis could also demonstrate unusual behavior in time-varying environments.

Many existing works on molecular ratchets focus on their dynamics with a given fixed energy landscape [10,22,27,28,32–40]. However, only recently has the *optimal design of the energy landscape* for functional molecular ratchets and pumps [41–44] been explored. This Letter focuses on identifying a different regime of driven catalysis and the corresponding design principles of its optimal energy landscape.

Consider a catalyst and a chemical reaction whose forward direction is always spontaneous for a continuous range of stationary temperatures. If temperature oscillates within the range, can the catalyst drive the reaction backward? If yes, the catalyst harnesses environmental energy to convert low

free-energy products to high free-energy reactants. Although counterintuitive, this effect is similar to Parrondo's paradox [45], where a gambler can win a game by periodically switching between two losing strategies.

This Letter derives a universal objective function to find the catalyst's energy landscape that can maximally drive the reaction against its spontaneous direction. The objective function [Eq. (13)] is simply related only to the activation energies in the catalytic cycle, shown as α_{ij} in Fig. 1. Thus, this theory is directly applicable to experimental selections of catalysts or designing catalytic reaction pathways to achieve energy harvesting.

Consider a general Markov model of the cyclic kinetics of catalysis sketched in Fig. 1, as a single-loop catalytic pathway consisting of N states. By completing a cycle, the reactant A is converted into product B, and the catalyst returns to its initial state. There are $2N$ transitions on the N-state cycle between adjacent states whose rates follow the Arrhenius law,

$$R_{ij} = r_{ij,0} \exp(-\beta \alpha_{ij}), \tag{1}$$

for state j to i. Here, β is the inverse temperature, and α_{ij} is the activation energy of the transition from j to i (see Fig. 1). The temperature-independent prefactor $r_{ij,0}$ can be proportional to the concentration of the external molecule (A or B) if an external molecule is absorbed in the transition.

The dynamics of the catalysis can be described by the master equation

$$\frac{d\vec{p}}{dt} = \hat{R}(\beta) \cdot \vec{p}, \tag{2}$$

where $\vec{p}$ is a N-dim column vector characterizing the probability of each state, $\hat{R}(\beta)$ is the transition rate matrix at given inverse temperature β, the off-diagonal elements of $\hat{R}$ are R_{ij}, and the diagonal elements are chosen such that each column of $\hat{R}$ sums to 0.
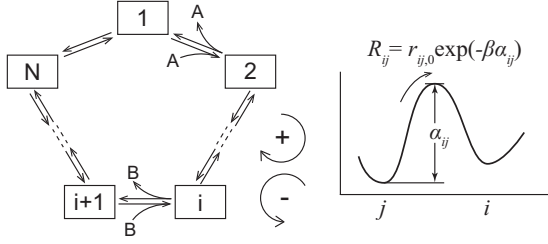
---

*zhiyuelu@unc.edu

FIG. 1. A general model of a catalyzed reaction, where the catalyst undergoes a cyclic pathway consisting of N intermediate states and $2N$ transitions. A and B represent the sets of reactants and products, which can join/leave the catalytic loop at arbitrary locations. We choose a convention that the forward reaction goes clockwise. The transition from j to i and its rate R_{ij} is illustrated by the energy landscape

Throughout this Letter, we assume that the chemical bath is infinitely large, so the chemical concentrations remain constant. Then at a fixed temperature, this system reaches a NESS, $\vec{p}^{ss}$ where $\hat{R}(\beta) \cdot \vec{p}^{ss} = 0$. Then the spontaneous reaction's rate is characterized by the net NESS probability current,

$$J^{ss} = R_{21} p_1^{ss} - R_{12} p_2^{ss}, \tag{3}$$

where at NESS, the current is uniform across the loop, and we choose to define it between states 1 and 2. In this work, we choose the convention that clockwise (CW) current is positive, corresponding to the forward reaction (A to B), and the counterclockwise (CCW) current is negative. If the Gibbs free energy of A is higher than B ($G_A > G_B$), the forward reaction is spontaneous, leading to a positive NESS current $J^{ss} > 0$. The affinity, which is equal to the free-energy difference between A and B, determines the direction,

$$\mathcal{A} \equiv \beta^{-1} \sum_{\langle i,j \rangle} \varepsilon_{ij} \ln R_{ij} = G_A - G_B = -\Delta G, \tag{4}$$

where ΔG is the free-energy change corresponding to the forward reaction, and the $\sum_{\langle i,j \rangle}$ sums over all of the $2N$ transitions from j to i on the loop. We have adopted the following sign indicator of a transition from j to i:

$$\varepsilon_{ij} = \begin{cases} 1 & \text{forward,} \\ -1 & \text{backward.} \end{cases} \tag{5}$$

If $\mathcal{A} > 0$, the spontaneous reaction is forward, $\mathcal{A} < 0$ backward, and if $\mathcal{A} = 0$, the system is at thermal equilibrium without net reaction flow. In this Letter, we assume G_A is always greater than G_B within the temperature range of interest, and thus $\mathcal{A} > 0$ and $J^{ss} > 0$, and the spontaneous reaction always goes forward (CW).

If the temperature nonquasistatically oscillates in time, the chemical reaction is driven out of NESS. The system eventually reaches a time-periodic state (i.e., a periodic orbit in probability space), $\vec{p}(t + \tau) = \vec{p}(t)$, where τ is the period of temperature oscillation. There have been studies of the periodic states under periodic temperature modulation [29,30]. However, it is generally impossible to analytically solve the dynamics for arbitrary systems or arbitrary reaction landscapes. To derive the generic design principle, in this Letter, we consider the *fast oscillation limit* $\tau \to 0$ [46], where a perturbation analysis [47] for small periods τ could reveal an analytical solution of the periodic orbit shrinking into a fixed point $\vec{p}(t) \to \vec{p}^*$, which leads to a general principle that applies to arbitrary reaction energy landscapes. [See Supplemental Material (SM) Sec. I [48].] The fixed point $\vec{p}^*$ can be considered as an *effective NESS* corresponding to an *effective rate matrix* $\hat{R}^*$,

$$\hat{R}^* \cdot \vec{p}^* = 0, \tag{6}$$

where the effective rate matrix is merely the time average of $\hat{R}(\beta(t))$ over a period:

$$\hat{R}^* \equiv \lim_{\tau \to 0} \frac{1}{\tau} \int_0^\tau \hat{R}(\beta(t)) dt. \tag{7}$$

At the fast oscillation limit, one can find the average current by using $\vec{p}^*$ and $\hat{R}^*$ similar to that in Eq. (3):

$$J^* = R_{21}^* p_1^* - R_{12}^* p_2^*. \tag{8}$$

In contrast to NESS, the affinity is no longer well defined since the temperature is no longer a fixed constant. Here, without a constant temperature, we introduce an *dimensionless affinity*,

$$\tilde{\mathcal{A}} = \sum_{\langle i,j \rangle} \varepsilon_{ij} \ln R_{ij}, \tag{9}$$

where R_{ij} is not restricted to a fixed-temperature rate matrix $\hat{R}(\beta)$ but can also be defined for the effective rate matrix $\hat{R}^*$. At a constant temperature, the $\tilde{\mathcal{A}}$ calculated from a stationary temperature rate matrix $\hat{R}(\beta)$ can be related back to $\mathcal{A}$ by $\tilde{\mathcal{A}} = \beta \mathcal{A}(\beta) = -\beta \Delta G$. When temperature rapidly oscillates, one can define the effective dimensionless affinity $\tilde{\mathcal{A}}^*$ by plugging the effective rate matrix $\hat{R}^*$ in Eq. (9).

Under oscillatory temperature, the direction of reaction (the sign of J^*) is solely determined by the active driving force $\tilde{\mathcal{A}}^*$: If $\tilde{\mathcal{A}}^* > 0$, the reaction on average proceeds forward ($J^* > 0$); if $\tilde{\mathcal{A}}^* < 0$, the reaction on average proceeds backward ($J^* < 0$).

Thus, the goal of searching for a catalyst to invert a spontaneous reaction is formulated in terms of $\tilde{\mathcal{A}}^*$: Consider a spontaneous reaction where $\Delta G < 0$, $J(\beta) > 0$, and $\tilde{\mathcal{A}}(\beta) > 0$ for any temperature within a continuous range. When temperature oscillates within the range, what catalyst facilitates a negative $\tilde{\mathcal{A}}^* < 0$ (i.e., the reaction is inverted and $J^* < 0$)?

In this Letter, based on the geometric properties of $\tilde{\mathcal{A}}$, we obtain a universal objective function, Eq. (13), to find the optimal catalytic reaction inversion. Historically, geometry has played important roles in thermodynamics. Gibbs first used geometry to demonstrate the thermodynamic properties within the space of state functions [49]. Recently, Crooks [50], Ito [51,52], and Dong [53] have derived various general thermodynamic results by utilizing differential geometry within various types of probability-distribution spaces.

Rather than working within a probability space, this Letter focuses on the geometry in the $2N$-dimensional space consisting of kinetic rates: $\mathbf{r} = (R_{21}, R_{12}, \ldots, R_{ji}, R_{ij}, \ldots, R_{1N}, R_{N1})$. According to Eq. (1), the reaction rates are determined by both temperature β^{-1} and the catalytic energy landscape α_{ij}'s. For any catalyst specified by its energy landscape α_{ij}'s, its kinetic rates $\mathbf{r}(\beta)$
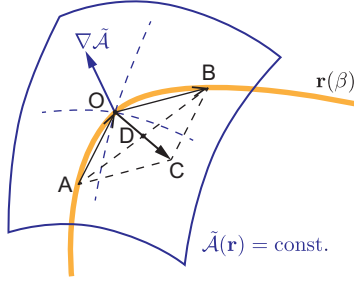
FIG. 2. The $2N$-dimensional design space of $\mathbf{r} = (R_{21}, R_{12}, \ldots, R_{ji}, R_{ij}, \ldots, R_{1N}, R_{N1})$. The yellow β locus crossing three points AOB is the set of $\mathbf{r}(\beta)$ corresponding to a given energy landscape at all possible inverse temperature β's. The blue surface represents a $(2N - 1)$ manifold defined by $\tilde{\mathcal{A}}(\mathbf{r}) = \text{const}$ that contains point O. The gradient of $\tilde{\mathcal{A}}(\mathbf{r})$ at point O is shown as the blue normal vector $\nabla\tilde{\mathcal{A}}$. When we consider temperature oscillation between $\beta_{1,2} = \beta_0 \pm \Delta\beta$, their corresponding rate matrices are points A and B. The rate matrix at β_0 is represented by point O. The effective rate matrix $\hat{R}^*$ corresponds to the midpoint D between A and B. At infinitesimal temperature amplitude, the vector $\overrightarrow{OC} = \overrightarrow{OB} - \overrightarrow{AO}$ becomes $d^2\mathbf{r}/d\beta^2$ in Eq. (11).

parametrized by inverse temperature β are illustrated by a yellow β locus in Fig. 2.

Without losing generality, let us illustrate our theory using a simple square-wave temperature oscillation between β_1 and β_2 of equal time duration. At constant temperature, β_1 (or β_2), the kinetic rate matrix $\hat{R}(\beta)$ or equivalently $\mathbf{r}(\beta)$ is illustrated by the point A (or B) on the β locus in Fig. 2. Under fast temperature oscillation, the effective rate matrix is simply the arithmetic mean,

$$\hat{R}^* = \frac{\hat{R}(\beta_1) + \hat{R}(\beta_2)}{2}, \tag{10}$$

and is represented by point D, the midpoint between A and B in the $\mathbf{r}$ space.

Recall that the generalized dimensionless affinity $\tilde{\mathcal{A}}(\mathbf{r})$ is a function on the $\mathbf{r}$ space, and its sign dictates the direction of averaged flow. By construction, within the range of $\beta \in [\beta_1, \beta_2]$, the reaction free energy $\Delta G(\beta) < 0$ and $\tilde{\mathcal{A}}(\mathbf{r}(\beta)) > 0$. Typically, point D is not on the yellow locus $\mathbf{r}(\beta)$. Thus $\tilde{\mathcal{A}}(\mathbf{r})$ at point D can take a very different value than that on the yellow locus. When $\tilde{\mathcal{A}}(\mathbf{r}) < 0$ at point D, the catalyst inverts the reaction direction when temperature oscillates rapidly.

Geometrically, the catalyst is represented by a locus $\mathbf{r}(\beta)$ in the $\mathbf{r}$ space. The analysis above allows us to characterize the catalyst's ability to invert the reaction by how much the locus $\mathbf{r}(\beta)$ curves toward the steepest descent direction (gradient) of $\tilde{\mathcal{A}}(\mathbf{r})$. Notice this geometrical characterization is not dependent on the specific protocol of temperature oscillation.

The qualitative geometrical argument above can be quantified by two vectors. First, the bending of the β locus $\mathbf{r}(\beta)$ can be characterized by the second-order derivative vector $d^2\mathbf{r}/d\beta^2$ (see vector $\overrightarrow{OC}$ in Fig. 2). This curvaturelike vector is the acceleration vector for the motion of point $\mathbf{r}(\beta)$ as the β varies. The entries of $d^2\mathbf{r}/d\beta^2$ are

$$\frac{d^2R_{ij}}{d\beta^2} = \alpha_{ij}^2 R_{ij}. \tag{11}$$
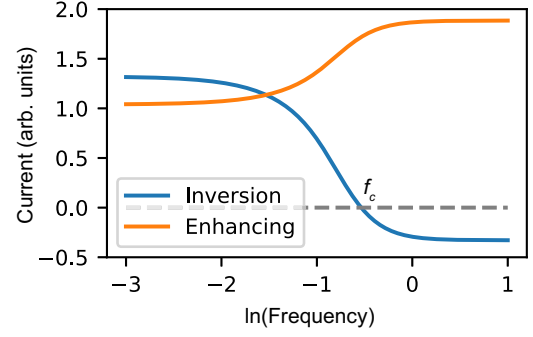

FIG. 3. Reaction rate (average probability current at periodic steady state) vs temperature oscillation frequency $f = \tau^{-1}$ for both the optimal energy landscapes for reaction inversion and enhancement, obtained for $\mathcal{A} = -\Delta G = 1$, $\alpha_{\max} = 11$, $\beta_0 = 0.9$, and $\Delta\beta = 0.3$.

Second, the variation of $\tilde{\mathcal{A}}$ in the $\mathbf{r}$ space is characterized by the gradient vector $\nabla\tilde{\mathcal{A}}(\mathbf{r})$ (as the blue arrow in Fig. 2), whose entries are

$$\frac{\partial\tilde{\mathcal{A}}}{\partial R_{ij}} = \frac{\varepsilon_{ij}}{R_{ij}}. \tag{12}$$

Combining the above, the catalyst's ability to invert the reaction direction is characterized by the inner product between the second-order derivative vector $d^2\mathbf{r}/d\beta^2$ and the gradient vector of $\tilde{\mathcal{A}}$,

$$\mathcal{C}(\{\alpha_{ij}\}) = \nabla\tilde{\mathcal{A}} \cdot \frac{d^2\mathbf{r}}{d\beta^2} = \sum_{\langle i,j \rangle} \varepsilon_{ij}\alpha_{ij}^2, \tag{13}$$

which serves as a universal objective function to find the optimal catalytic energy landscape that can achieve strong reaction inversion.

An alternative derivation based on a finite-difference analysis of temperature oscillation between $\beta_0 - \Delta\beta$ and $\beta_0 + \Delta\beta$ is shown in Fig. 2 and the SM (see SM Sec. II [48]). Here, $\mathcal{C}(\{\alpha_{ij}\})$ is directly proportional to $\Delta\tilde{\mathcal{A}}$, the difference of $\tilde{\mathcal{A}}$ of $\hat{R}^*$, and the NESS $\tilde{\mathcal{A}}(\beta_0)$ at constant temperature β_0,

$$\Delta\tilde{\mathcal{A}} \equiv \tilde{\mathcal{A}}(\hat{R}^*) - \tilde{\mathcal{A}}(\mathbf{r}(\beta_0)) = \mathcal{C}(\{\alpha_{ij}\})\frac{\Delta\beta^2}{2} + o(\Delta\beta^2). \tag{14}$$

Due to the nice geometric properties of the constant-$\tilde{\mathcal{A}}(\mathbf{r})$ manifold and the β locus [54], the R_{ij} from Eqs. (11) and (12) cancels out, and the resulting objective function Eq. (13) takes a simple quadratic form that only depends on the activation energies of the catalyst α_{ij}'s, and is independent of the specific temperature protocol. For the same geometrical reason, $\mathcal{C}$ applies to large-amplitude temperature oscillation [see Fig. 4(b)].

The objective function $\mathcal{C}(\{\alpha_{ij}\})$ is directly accessible by experiment via direct measurements of the activation energies α_{ij}'s. Thus, our result [Eq. (13)] provides an easy approach to predict the arbitrary catalysts' ability to invert reaction direction under fast temperature oscillation.

For illustration, Fig. 3 demonstrates the frequency response of the optimal three-state catalyst landscape ($\{\alpha_{ij}\}$) under the following design constraints. First, we fix the reaction's free-energy change $\Delta G(\beta) = -1$ for all β's. As a result, the affinity must be constant $\mathcal{A} = -\Delta G = 1$ regardless of the
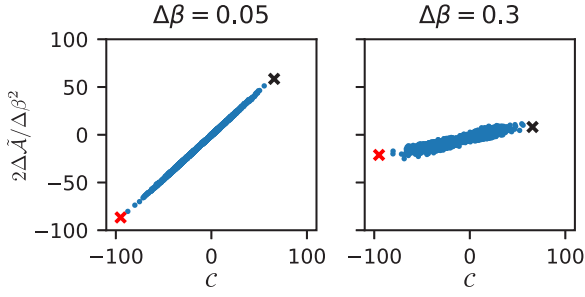
FIG. 4. Objective function $\mathcal{C}$ and the scaled affinity change $2\Delta\tilde{A}/\Delta\beta^2$ for randomly generated energy landscapes under the same set restriction with the optimization problem ($\mathcal{A} = -\Delta G = 1$, $\alpha_{\max} = 11$, $\beta_0 = 0.9$). The red and black crosses correspond to the optimal energy landscapes for reaction inversion (minimizing $\mathcal{C}$) and enhancement (maximizing $\mathcal{C}$).

choice of the catalyst. Second, we assume that the reaction rate prefactor $r_{ij,0}$'s are all fixed to be the same constant. By doing so for any constant temperature,

$$\mathcal{A} = -\sum_{+} \alpha_{ij} + \sum_{-} \alpha_{ij} = 1, \tag{15}$$

where $\sum_{+}$ (or $\sum_{+}$) is the sum over all forward (or backward) reaction transitions. Third, as we search for the optimal landscape (activation energies), we restrict the activation energies of all $2N$ transitions in the range $\alpha_{ij} \in [0, \alpha_{\max}]$. Here, we assume the reaction's affinity is weaker than the maximum allowed activation energy: $\mathcal{A} = 1 < \alpha_{\max}$.

According to our result, to find the optimal catalyst with the strongest driving force against spontaneous reaction under temperature oscillation, one needs to minimize the objective function

$$\mathcal{C} = \sum_{+} \alpha_{ij}^2 - \sum_{-} \alpha_{ij}^2, \tag{16}$$

which is a simple quadratic minimization problem on a convex set. For $N = 3$, the optimal solution of α_{ij}'s are

$$\alpha_{+}^{\mathrm{inv}} = \left(\frac{2\alpha_{\max} - 1}{3}, \frac{2\alpha_{\max} - 1}{3}, \frac{2\alpha_{\max} - 1}{3} \right), \tag{17}$$

$$\alpha_{-}^{\mathrm{inv}} = (\alpha_{\max}, \alpha_{\max}, 0), \tag{18}$$

where $\alpha_{+}^{\mathrm{inv}}$ are the activation energies α_{ij}'s for the three forward transitions and $\alpha_{-}^{\mathrm{inv}}$ are for the three backward transitions (see SM Sec. IV [48]). The order of the three forward (or three backward) α_{ij}'s does not impact the result.

Beyond the fast oscillation limit, the optimal catalyst can invert the reaction at finite frequency f's (see Fig. 3). At the critical frequency $f = f_c$, the reaction free-energy force ΔG is completely stalled by inversion force from the catalyst, and the reaction stops ($J_{\mathrm{period}} = 0$); at larger frequency $f > f_c$, the catalyst's driving wins over ΔG and reaction direction is inverted ($J_{\mathrm{period}} < 0$). At the fast oscillation limit $f \gg 1$, we can use the matrix tree theorem [55] to obtain from the effective rate matrix R^* the effective current $J^* = (R_{13}^* R_{32}^* R_{21}^* - R_{12}^* R_{23}^* R_{31}^*)/\kappa$, where $\kappa > 0$ (see SM Sec. III [48]). Thus the sign of current J^* is always the same as that of $\tilde{A}^*$.

It is worth pointing out that the objective function Eq. (13) can be used toward an inverse effect of catalytic reaction

inversion, i.e., driving force enhancing. By maximizing Eq. (13) (see SM Sec. IV [48]),

$$\alpha_{+}^{\mathrm{enh}} = (\alpha_{\max}, \alpha_{\max}, 0), \tag{19}$$

$$\alpha_{-}^{\mathrm{enh}} = \left(\frac{2\alpha_{\max} + 1}{3}, \frac{2\alpha_{\max} + 1}{3}, \frac{2\alpha_{\max} + 1}{3} \right) \tag{20}$$

defines a reaction-enhancing catalyst that optimally enhances the spontaneity of a reaction. The reaction current enhanced at various frequencies f is shown in Fig. 3.

Even though $\mathcal{C}$ [Eq. (13)] is obtained from the local curvature, due to nice geometric properties of $\tilde{A}(\mathbf{r})$ and $\mathbf{r}(\beta)$, it remains a good optimization objective function even for large-amplitude temperature oscillations (e.g., for $\beta_0 = 0.9$, $\Delta\beta = 0.3$). We demonstrate that for both small and large amplitudes, $\mathcal{C}$ is approximately linearly correlated to the change of thermodynamic driving force. The linear correlation is shown in Fig. 4 for both small $\Delta\beta = 0.05$ and large $\Delta\beta = 0.3$ by scatter plots of 10^4 points. Each point is obtained from one randomly generated energy landscape $\{\alpha_{ij}\}$. Notice in the small-amplitude limit, $\Delta\beta \ll 1$, $\mathcal{C}$ is equal to $2\Delta\tilde{A}/\Delta\beta^2$ [Eq. (14)]. The optimal catalysts for reaction inversion and enhancement (obtained by minimizing and optimizing $\mathcal{C}$) are highlighted as red and black crosses, appearing at the two ends of both scatter plots.

At stationary temperature, kinetic intuition may argue that the higher the activation energy, the slower are the corresponding transition rates. However, when temperature oscillates, our theory indicates that a big variation in the activation energies of the inverse reaction direction and mild activation energies of the forward reaction direction could suppress the forward reaction and favor the inverse direction. Moreover, designing the catalytic reaction inversion suffers from a trade-off relation between strength and speed. Strong inversion (large $|\Delta\tilde{A}|$) favors the choice of larger activation energies (larger α_{ij}), which impedes the net reaction current.

In conclusion, this Letter demonstrated a geometric approach to derive the general design principle of optimal oscillatory-driven catalysis. In this regime, we demonstrate catalysts that can harness energy from an oscillatory-temperature bath and utilize the energy to enhance or invert a spontaneous reaction. The design principle is formulated by an objective function Eq. (13), which only depends on the activation energies of the energy landscape in a quadratic form. Due to the nice geometric properties of the thermodynamic driving force $\tilde{A}$, the objective function is independent of the temperature protocol. Moreover, this result obtained from the fast oscillation limit can still be used to invert spontaneous reactions at finite-frequency temperature oscillation. Since activation energies are accessible in the experimental study of reaction mechanisms, this result could be experimentally verified and directly used to guide the design of useful catalysts for energy harnessing.

[1] H. V. Westerhoff, T. Y. Tsong, P. Chock, Y.-D. Chen, and R. Astumian, How enzymes can capture and transmit free energy from an oscillating electric field, Proc. Natl. Acad. Sci. USA **83**, 4734 (1986).

[2] V. Rozenbaum, D.-Y. Yang, S. Lin, and T. Tsong, Catalytic wheel as a Brownian motor, J. Phys. Chem. B **108**, 15880 (2004).

[3] H. Qian, Cycle kinetics, steady state thermodynamics and motors—a paradigm for living matter physics, J. Phys.: Condens. Matter **17**, S3783 (2005).

[4] R. D. Astumian, Making molecules into motors, Sci. Am. **285**, 56 (2001).

[5] R. Yasuda, H. Noji, M. Yoshida, K. Kinosita, Jr., and H. Itoh, Resolution of distinct rotational substeps by submillisecond kinetic analysis of F_1-ATPase, Nature (London) **410**, 898 (2001).

[6] T. L. Hill and Y.-D. Chen, Stochastics of cycle completions (fluxes) in biochemical kinetic diagrams, Proc. Natl. Acad. Sci. USA **72**, 1291 (1975).

[7] H. Qian, A simple theory of motor protein kinetics and energetics, Biophys. Chem. **67**, 263 (1997).

[8] H. Qian, A simple theory of motor protein kinetics and energetics. II, Biophys. Chem. **83**, 35 (2000).

[9] R. D. Astumian and P. Hänggi, Brownian motors, Phys. Today **55** (11), 33 (2002).

[10] P. Reimann, Brownian motors: Noisy transport far from equilibrium, Phys. Rep. **361**, 57 (2002).

[11] T. L. Hill, *Free Energy Transduction and Biochemical Cycle Kinetics* (Courier Corporation, North Chelmsford, MA, 2013).

[12] Y.-D. Chen, Asymmetry and external noise-induced free energy transduction, Proc. Natl. Acad. Sci. USA **84**, 729 (1987).

[13] T. Tsong and R. D. Astumian, Electroconformational coupling: How membrane-bound atpase transduces energy from dynamic electric fields, Annu. Rev. Physiol. **50**, 273 (1988).

[14] O. Raz, Y. Subaşı, and C. Jarzynski, Mimicking Nonequilibrium Steady States with Time-Periodic Driving, Phys. Rev. X **6**, 021022 (2016).

[15] D. M. Busiello, C. Jarzynski, and O. Raz, Similarities and differences between non-equilibrium steady states and time-periodic driving in diffusive systems, New J. Phys. **20**, 093015 (2018).

[16] R. D. Astumian and M. Bier, Fluctuation driven ratchets: Molecular motors, Phys. Rev. Lett. **72**, 1766 (1994).

[17] J. M. Horowitz and C. Jarzynski, Exact formula for currents in strongly pumped diffusive systems, J. Stat. Phys. **136**, 917 (2009).

[18] O. Abah, J. Roßnagel, G. Jacob, S. Deffner, F. Schmidt-Kaler, K. Singer, and E. Lutz, Single-Ion Heat Engine at Maximum Power, Phys. Rev. Lett. **109**, 203006 (2012).

[19] R. D. Astumian, Design principles for Brownian molecular machines: How to swim in molasses and walk in a hurricane, Phys. Chem. Chem. Phys. **9**, 5067 (2007).

[20] S. Rahav, J. Horowitz, and C. Jarzynski, Directed Flow in Nonadiabatic Stochastic Pumps, Phys. Rev. Lett. **101**, 140602 (2008).

[21] N. Sinitsyn and I. Nemenman, The Berry phase and the pump flux in stochastic chemical kinetics, Europhys. Lett. **77**, 58001 (2007).

[22] R. D. Astumian, Adiabatic operation of a molecular machine, Proc. Natl. Acad. Sci. USA **104**, 19715 (2007).

[23] R. D. Astumian, Adiabatic Pumping Mechanism for Ion Motive ATPases, Phys. Rev. Lett. **91**, 118102 (2003).

[24] R. D. Astumian and I. Derényi, Towards a Chemically Driven Molecular Electron Pump, Phys. Rev. Lett. **86**, 3859 (2001).

[25] J. M. R. Parrondo, Reversible ratchets as Brownian particles in an adiabatically changing periodic potential, Phys. Rev. E **57**, 7297 (1998).

[26] R. D. Astumian, Stochastically pumped adaptation and directional motion of molecular machines, Proc. Natl. Acad. Sci. USA **115**, 9405 (2018).

[27] Y.-X. Li, Transport generated by fluctuating temperature, Physica A **238**, 245 (1997).

[28] P. Reimann, R. Bartussek, R. Häussler, and P. Hänggi, Brownian motors driven by temperature oscillations, Phys. Lett. A **215**, 26 (1996).

[29] H. Berthoumieux, L. Jullien, and A. Lemarchand, Response to a temperature modulation as a signature of chemical mechanisms, Phys. Rev. E **76**, 056112 (2007).

[30] A. Lemarchand, H. Berthoumieux, L. Jullien, and C. Gosse, Chemical mechanism identification from frequency response to small temperature modulation, J. Phys. Chem. A **116**, 8455 (2012).

[31] H. Berthoumieux, C. Antoine, L. Jullien, and A. Lemarchand, Resonant response to temperature modulation for enzymatic dynamics characterization, Phys. Rev. E **79**, 021906 (2009).

[32] I. Derényi, M. Bier, and R. D. Astumian, Generalized Efficiency and its Application to Microscopic Engines, Phys. Rev. Lett. **83**, 903 (1999).

[33] I. Derényi and R. D. Astumian, Efficiency of Brownian heat engines, Phys. Rev. E **59**, R6219 (1999).

[34] B.-Q. Ai, H.-Z. Xie, D.-H. Wen, X.-M. Liu, and L.-G. Liu, Heat flow and efficiency in a microscopic engine, Eur. Phys. J. B **48**, 101 (2005).

[35] U. Seifert, Stochastic thermodynamics, fluctuation theorems and molecular machines, Rep. Prog. Phys. **75**, 126001 (2012).

[36] J. Parrondo and B. J. de Cisneros, Energetics of Brownian motors: A review, Appl. Phys. A **75**, 179 (2002).

[37] K. Sekimoto, F. Takagi, and T. Hondou, Carnot's cycle for small systems: Irreversibility and cost of operations, Phys. Rev. E **62**, 7759 (2000).

[38] T. Hondou and K. Sekimoto, Unattainability of Carnot efficiency in the Brownian heat engine, Phys. Rev. E **62**, 6021 (2000).

[39] M. Asfaw and M. Bekele, Current, maximum power and optimized efficiency of a Brownian heat engine, Eur. Phys. J. B **38**, 457 (2004).

[40] C. Van den Broeck, Carnot efficiency revisited, in *Special Volume in Memory of Ilya Prigogine*, edited by S. A. Rice, Advances in Chemical Physics Vol. 135 (Wiley, Hoboken, NJ, 2007), Chap. 6, pp. 189–201.

[41] A. I. Brown and D. A. Sivak, Toward the design principles of molecular machines, La Phys. Au Canada, **73**, 61 (2017).

[42] J. N. E. Lucero, A. Mehdizadeh, and D. A. Sivak, Optimal control of rotary motors, Phys. Rev. E **99**, 012119 (2019).

[43] A. I. Brown and D. A. Sivak, Theory of nonequilibrium free energy transduction by molecular machines, Chem. Rev. **120**, 434 (2020).

[44] A. I. Brown and D. A. Sivak, Allocating and splitting free energy to maximize molecular machine flux, J. Phys. Chem. B **122**, 1387 (2018).

[45] G. P. Harmer and D. Abbott, Losing strategies can win by Parrondo's paradox, Nature (London) **402**, 864 (1999).

[46] Although the optimal design principle is derived under the fast oscillation limit, Fig. 3 indicates that the optimal catalyst here is able to invert reaction direction even under finite driving frequencies.

[47] M. Tagliazucchi, E. A. Weiss, and I. Szleifer, Dissipative self-assembly of particles interacting through time-oscillatory potentials, Proc. Natl. Acad. Sci. USA **111**, 9751 (2014).

[48] See Supplemental Material at http://link.aps.org/supplemental/10.1103/PhysRevE.107.L012102 for the alternative derivation of the theory and supplemental evidence.

[49] F. Weinhold, Thermodynamics and geometry, Phys. Today **29** (3), 23 (1976).

[50] D. A. Sivak and G. E. Crooks, Thermodynamic Metrics and Optimal Paths, Phys. Rev. Lett. **108**, 190602 (2012).

[51] S. Ito, Stochastic Thermodynamic Interpretation of Information Geometry, Phys. Rev. Lett. **121**, 030605 (2018).

[52] K. Yoshimura and S. Ito, Information geometric inequalities of chemical thermodynamics, Phys. Rev. Res. **3**, 013175 (2021).

[53] G. Li, J.-F. Chen, C. P. Sun, and H. Dong, Geodesic Path for the Minimal Energy Cost in Shortcuts to Isothermality, Phys. Rev. Lett. **128**, 230603 (2022).

[54] In the logarithmic $\mathbf{r}$ space, the constant-$\tilde{\mathcal{A}}$ manifolds become a set of parallel hyperplanes with unidirectional gradients, and the β locus for any energy landscape is a straight line. The gradient of $\tilde{\mathcal{A}}$ and the acceleration vector of the β locus has an elementarywise inverse dependence on R_{ij}.

[55] J. Schnakenberg, Network theory of microscopic and macroscopic behavior of master equation systems, Rev. Mod. Phys. **48**, 571 (1976).